

JCTC

Journal of Chemical Theory and Computation

Quantum-Chemical Design of Cryptand-like Ditopic Salt Binders

Siân T. Howard,^{*,†} David E. Hibbs,^{*,‡} Angelo J. Amoroso,[§] and James A. Platts[§]

School of Pharmacy and Medical Sciences, University of South Australia, Adelaide, South Australia 5000, Australia, Faculty of Pharmacy, University of Sydney, Camperdown, New South Wales 2006, Australia, and Department of Chemistry, Cardiff University, Cardiff CF10 3TB, Wales, U.K.

Received November 6, 2005

Abstract: Hartree–Fock, density functional, and MP2 methods are applied to the problem of designing neutral, bicyclic C_3 -symmetric cages incorporating interacting anion- and cation-binding sites which strongly bind NaCl as an ion contact pair. A large number of trial ligands **L** and their complexes **L**:NaCl are tested, with the focus on maximizing binding by (i) optimizing the cavity size and shape and (ii) varying the nature of the anion- and cation-binding functionalities. The corresponding complexes **L**:Cl[−] and **L**:Na⁺ are also studied in some detail. An analysis of their structures and charge distributions helps to build a consistent picture of the requirements for a successful NaCl binding. The ‘best’ candidate ligand utilizes a tripodal triether-substituted amine N(CH₂CH₂OR)₃ to bind the sodium cation; three thiourea groups in a tripodal arrangement with a 1,3,5-trisubstituted benzyl spacer group {C₆H₃(CH₂NHC=XNH)₃ X=O,S} to bind chloride; and a –CH₂CH₂– spacer linking the two binding sites. A simple Quantitative Structure–Property analysis suggests that the binding cavity shape and size is near to the optimal one for this system.

Introduction

One of the emerging fields of interest in supramolecular chemistry is the recognition of ion pairs.^{1,2} The key idea embodied in the design of appropriate multisite receptors is one of cooperativity, i.e., that the binding of one ion might facilitate either stronger or more selective binding of the other. Moreover, because a neutral host ligand incorporating an ion pair M^+X^- provides an overall uncharged system, for biochemical applications the transport properties of such neutral ditopic binders across lipophilic membranes might be superior. Sodium ions and chloride ions are the dominant cationic and anionic species in human interstitial fluid.³ Chloride transport disfunction is associated with a number of disease states including cystic fibrosis.⁴ A synthetic host

which selectively binds chloride and can pass across cell membranes might therefore have therapeutic possibilities⁵ or could be used in a chloride assay. A molecule which binds NaCl selectively and reversibly could also form the basis of a *chemical* desalination/purification process for drinking water.

Suitable ditopic receptors might be classified into two broad categories: (i) those which bind a given pair of ions at sites remote from each other, such as the calixarene-based **A** (see Chart 1) due to Reinhoudt and co-workers⁶ or (ii) ion contact pair binders such as the diamide-functionalized crown ether **B** (see Chart 1) recently reported by Smith et al.^{7,8} The latter binds NaCl, KCl, and various trigonal anion combinations such as KNO₃. Moreover it has been shown to be capable of transporting the bound ion pair across a vesicle membrane.⁷

In a simplistic picture of macrocyclic ditopic receptor design (see Scheme 1) we can identify five types of elements: the anion binding sites (AB) and the anion binder cap; the cation binding sites (CB) and the cation binder cap;

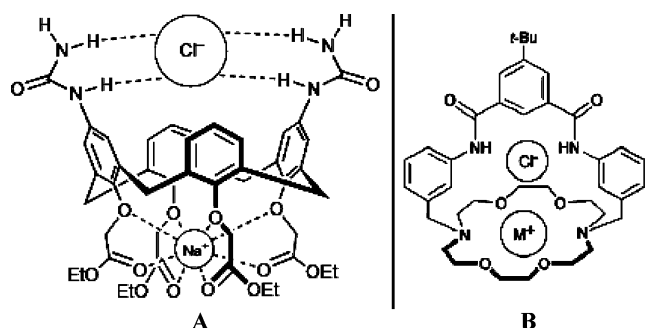
* Corresponding author phone: 61883021944; fax: 61883022389; e-mail: sian.howard@unisa.edu.au (S.T.H.).

[†] University of South Australia.

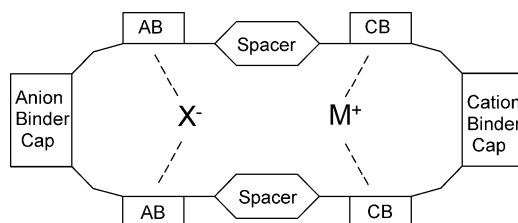
[‡] University of Sydney.

[§] Cardiff University.

Chart 1



Scheme 1

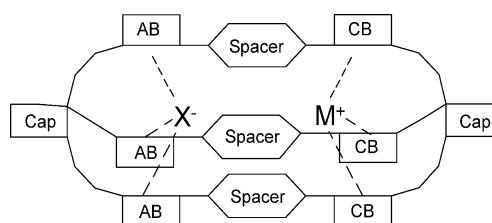


and the spacer or linker group between them. In general we might reasonably assume that a long spacer will lead to a type A system with the anion and cation bound separately and not as an ion contact pair.

In the design of new ditopic receptors, it seems clear that modeling and simulation techniques at various levels of theory have tremendous potential for quantifying the binding strength of anion and cation sites and the effect of a given spacer element on $X^- \cdots M^+$ interactions and cooperative binding effects. Yet surprisingly, this is virgin territory in the quantum chemistry literature. Although a small number of quantum-chemical studies on anion binders have appeared in recent years,^{9–16} to date just one paper has appeared on ditopic binders: the study of Geerlings et al.¹⁷ They presented dft calculations on charged tin-containing crown ether-based host species capable of simultaneously binding Na^+ or K^+ along with SCN^- at a remote site, i.e., a type A ditopic binder in our simple classification scheme. The aim of this work is a computational study of *neutral* hosts which bind a salt M^+X^- as an ion contact pair, to identify potential new ditopic binders. We also spend some time considering which quantum chemical technique(s) are most appropriate for this task. This study focuses on the design of an optimal ligand for a particular ion pair ($NaCl$) without considering the question of selectivity, which will be the topic of a subsequent paper.

As mentioned above, at least one successful $NaCl$ ditopic binder of type B has already been reported.^{7,8} Although this bicyclic molecule and its complex with $NaCl$ is small in terms of supramolecular chemistry, lacking any elements of symmetry it already represents a major challenge for high-level computational methods, where it is natural to take a ‘minimalist’ approach with respect to the system size and to utilize symmetry wherever possible. Initially we spent some time considering whether a small macrocyclic system such as the one shown schematically in Scheme 1 would have the desired properties. Invariably we found that a simple macrocycle either did not encapsulate the ion pair effectively,

Scheme 2

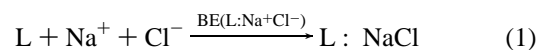


or the ions did not pair at all. This led us to focus on C_3 -symmetric bicyclic cryptand-like ligands, illustrated schematically in Scheme 2. This has several advantages: (i) the extra anion-binding site significantly increases anion binding, (ii) the bicycle more effectively encloses the ion pair (bound along the C_3 axis) which both reduces the likely role any solvent molecules would play and improves the likelihood of a size-selective mechanism, and (iii) the presence of a C_3 axis makes the calculations more efficient.

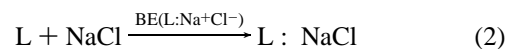
Computational Methods and Procedure

The complexes were initially modeled as $L:NaCl$ with approximate C_3 symmetry using the MM3+ force field in Macromodel.¹⁸ Low-level quantum mechanical (HF/3-21G) geometry optimizations were then performed in C_1 symmetry, followed by harmonic frequency analyses to check for stability. Complexes which either distorted from C_3 symmetry or gave one or more imaginary frequencies were rejected at this stage. The “successful” complexes were then precisely symmetrized, and subsequent geometry optimization was performed at the HF/6-31+G* and BHandH/6-31+G* levels of theory (the latter choice of density functional is rationalized later in the Results section). Gas-phase binding energies were calculated incorporating HF/3-21G harmonic thermal energy corrections (at 298 K) with the vibrational energy component scaled by 0.89.¹⁹ All calculations assumed singlet electronic ground states. Gaussian 03 was used for all quantum chemical calculations.²⁰

To measure the binding energies of a given L there are two clear choices: (i) binding energy relative to the separated ions, which we will call $BE(L:Na^+Cl^-)$, represented by the reaction



and (ii) binding energy relative to molecular $NaCl$, which we will denote as $BE(L:NaCl)$, represented by



In fact it does not much matter which one we use since they are related by a constant, which is (more or less) the energy required to form a gas-phase $NaCl$ molecule from the separated ions: $BE(L:Na^+Cl^-) = BE(L:NaCl) + D_o(NaCl)$.

For a given L, we can also measure its ability to separately bind Na^+ or Cl^- , i.e., the anion and cation affinities:



Table 1. Ground-State Spectroscopic Data for $^{23}\text{Na}^{35}\text{Cl}$

	r_e (Å)	ω_e (cm^{-1})	D_0 (kJ/mol) ^a
MP2/6-311+G*	2.382	367	547.7
HF/6-31+G*	2.406	351	531.2
B3LYP/6-31+G*	2.391	349	545.5
BHandH/6-31+G*	2.347	371	562.5
experiment ²¹	2.361	365	407.2

^a HF/3-21G zero-point energy scaled by 0.89¹⁸ used for all calculated values.

These binding energies are also of interest because (i) in solution all possible complexes $\text{L}:\text{NaCl}(\text{aq})$, $\text{L}:\text{Na}^+(\text{aq})$, and $\text{L}:\text{Cl}^-(\text{aq})$ would exist in equilibrium and (ii) knowing the magnitude of separate anion and cation affinities might help us to understand or interpret trends in the $\text{L}:\text{NaCl}$ ion pair binding energies. Hence three gas-phase binding energies (BEs) were subsequently computed for each L, requiring several additional calculations for each compound, including the “empty” ligand L and its complexes with Na^+ and Cl^- at HF/3-21G, HF/6-31+G*, and BHandH/6-31+G* levels of theory. Note that all gas-phase binding energies reported can be trivially converted to gas-phase binding enthalpies ΔH by adding an extra RT correction term (from $P\Delta V = \Delta nRT$ with $\Delta n=1$) ≈ 2.5 kJ/mol at 298 K.

Results

We begin by analyzing the structure and binding of a few model systems for which MP2 calculations are feasible, to establish whether HF theory or DFT would be most appropriate for these systems.

NaCl. Modeling NaCl tells us how a particular level of theory deals with the key $\text{X}^-\dots\text{M}^+$ interaction. Gas-phase structural data on the $^1\Sigma^+$ ground state of NaCl are known from vibronic spectroscopy.²¹ The calculations presented in Table 1 at four levels of theory shows that all of these (lower-level) methods considerably overestimate the binding energy of the molecule. BHandH and MP2 give the best bond length and vibrational frequency predictions (i.e. closest to experiment).

Complexes of *N,N'*-Dimethylurea (1a) and *N,N'*-Dimethylthiourea (1b) with Cl^- . As a model for one of the anion-binding moieties we use the symmetrically substituted molecule *N,N'*-dimethylurea **1a** and its thio-counterpart **1b** (Figure 1a,b). There appear to be no previous reports of calculations on these species (Frontera et al. have reported the MP2/6-311+G** structure and gas-phase binding energy for the urea: Cl^- complex^{14,22}). There are various subtleties associated with the conformations of gas-phase urea and thiourea;^{23,24} vibrational spectroscopy verifies C_2 symmetry for the lowest-energy conformations, but calculations give results which are strongly level and basis-set dependent. We find similar effects for the complexes of **1a** and **1b** and their complexes with Cl^- . **1a** is most stable in (nonplanar) C_2 symmetry at the HF/6-31+G* and BHandH/6-31+G* levels of theory. B3LYP/6-31+G* finds that **1a** is also stable C_s symmetry (unlike the other levels of theory). The urea complex **1a**: Cl^- (Table 2) is most stable in C_s symmetry for all levels of theory used with the exception of BHandH/6-

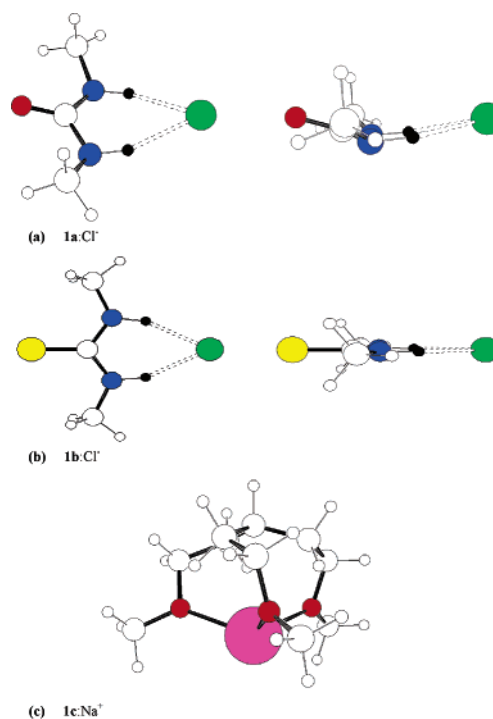


Figure 1. MP2-optimized geometries of model anion-bound and cation-bound complexes: (a) MP2/6-311+G** optimized Cl^- :dimethylurea complex (C_s), two perpendicular views; (b) MP2/6-311+G** optimized Cl^- :dimethylthiourea complex (C_s), two perpendicular views; (c) MP2/6-31+G* optimized $\text{H}(\text{CH}_2-\text{CH}_2\text{OMe})_3:\text{Na}^+$ complex (C_3).

Table 2. Properties of the *N,N'*-Dimethylurea... Cl^- Complex

	$r(\text{H}\cdots\text{Cl}^-)$ (Å)	$\text{N}-\text{H}\cdots\text{Cl}^-$ (deg)	BE (kJ/mol) ^a
MP2/6-311+G** (C_s)	2.241	159.5	110.1
HF/6-31+G* (C_s)	2.486	158.9	83.8
B3LYP/6-31+G* (C_s)	2.339	158.7	96.6
BHandH/6-31+G* (C_{2v})	2.224	158.0	123.4

^a Gas-phase binding energy including HF/3-21G thermal energies with the vibrational component scaled by 0.89.²¹

Table 3. Properties of the *N,N'*-Dimethylthiourea... Cl^- Complex

	$r(\text{H}\cdots\text{Cl}^-)$ (Å)	$\text{N}-\text{H}\cdots\text{Cl}^-$ (deg)	BE (kJ/mol) ^a
MP2/6-311+G** (C_{2v})	2.191	158.9	131.1
HF/6-31+G* (C_{2v})	2.414	160.4	109.8
B3LYP/6-31+G* (C_{2v})	2.282	159.3	119.9
BHandH/6-31+G* (C_{2v})	2.177	158.2	148.3

^a Gas-phase binding energy including HF/3-21G thermal energies with the vibrational component scaled by 0.89.²¹

31+G*, which prefers C_{2v} symmetry. The thiourea complex **1b**: Cl^- is most stable in C_{2v} symmetry for all levels of theory (Table 3).

It can be seen from the data in Tables 2 and 3 that HF/6-31+G* markedly underestimates the binding energies of **1a**: Cl^- and **1b**: Cl^- and also gives much longer $\text{N}-\text{H}\cdots\text{Cl}$ contact distances. The B3LYP/6-31+G* and BhandH/6-31+G* binding energies are lower and higher than the MP2 result by approximately the same amount, but the BhandH

Table 4. Properties of the Complex $\text{H}(\text{CH}_2\text{CH}_2\text{OMe})_3\text{Na}^+$

	$r(\text{O}\cdots\text{Na}^+)$ (Å)	$\text{C}-\text{O}\cdots\text{Na}^+$ (deg)	BE (kJ/mol) ^a
MP2/6-31+G* (C_3)	2.339	116.5	224.5
HF/6-31+G* (C_3)	2.291	118.2	219.6
B3LYP/6-31+G* (C_3)	2.283	117.3	227.4
BHandH/6-31+G* (C_3)	2.213	115.8	262.7

^a Gas-phase binding energy including HF/3-21G thermal energies with the vibrational component scaled by 0.89.²¹

optimized geometries are much closer to MP2 than the B3LYP results.

Complex of the Tripodal Podand $\text{HC}-(\text{CH}_2\text{CH}_2-\text{O}-\text{Me})_3$ with Na^+ . There have been a number of published studies of binding of alkali metal cations with e.g. crown ethers at the HF and MP2 levels of theory.²⁵ These have established that HF and MP2 give similar results for these systems, i.e., HF is a good model for cationic complexes of alkali metal ions. As a model for the common cation-binding moiety which is present in most of our ligands, we use the podand complex $\text{HC}(\text{CH}_2\text{CH}_2\text{OMe})_3\text{Na}^+$ (Figure 1c). In common with the previous studies of crown ether binding, the data in Table 2 show that HF provides a good approximation for both the geometry and binding energy of this type of complex; B3LYP is marginally poorer but still fairly close to the MP2 results. However, in this case BHandH overbinds the complex (compared to MP2) by 37 kJ/mol and correspondingly gives $\text{O}\cdots\text{Na}^+$ contact distances which are some 0.12 Å too short.

In summary: although the BHandH functional seems to be the best choice for the anion...cation interaction and the Cl^- ...urea/thiourea interaction, it is actually further from the MP2 binding energy or geometry than HF or B3LYP for the Na^+ ...ether interactions. Consequently in what follows, we present a full set of results at both HF/6-31+G* and BhandH/6-31+G* levels of theory. As a rule of thumb, we suggest that the BHandH data provide the most reliable geometries, but the “true” gas phase binding energy is bracketed by the HF and BHandH results (since these seem to consistently underestimate and overestimate binding compared to MP2, respectively).

Table 5. Composition of the Various Ditopic Binders

	anion binder cap	anion-binding moiety	spacer	cation-binding moiety	cation binder cap
1	HCR ₃	$-\text{CH}_2\text{CONH}-$	$-\text{CH}_2\text{CH}_2\text{CH}_2-$	$-\text{OCH}_2\text{CH}_2-$	R ₃ CH
2	HCR ₃	$-\text{CH}_2\text{CSNH}-$	$-\text{CH}_2\text{CH}_2\text{CH}_2-$	$-\text{OCH}_2\text{CH}_2-$	R ₃ CH
3	HCR ₃	$-\text{NHCONH}-$	$-\text{CH}_2\text{CH}_2\text{CH}_2-$	$-\text{OCH}_2\text{CH}_2-$	R ₃ CH
4	HCR ₃	$-\text{CH}_2\text{NHCONH}-$	$-\text{CH}_2\text{CH}_2-$	$-\text{OCH}_2\text{CH}_2-$	R ₃ CH
5	BzR ₃	$-\text{CH}_2\text{NHCONH}-$	$-\text{CH}_2\text{CH}_2-$	$-\text{OCH}_2\text{CH}_2-$	R ₃ CH
6	BzR ₃	$-\text{CH}_2\text{NHCSNH}-$	$-\text{CH}_2\text{CH}_2-$	$-\text{OCH}_2\text{CH}_2-$	R ₃ CH
7	BzR ₃	$-\text{CH}_2\text{CH}_2\text{NHCSNH}-$	$-\text{CH}_2\text{CH}_2-$	$-\text{OCH}_2\text{CH}_2-$	R ₃ CH
8	BzR ₃	$-\text{CH}_2\text{CH}_2\text{NHCONH}-$	$-\text{CH}_2\text{CH}_2-$	$-\text{OCH}_2\text{CH}_2-$	R ₃ CH
9		$\text{H}_3\text{C}-\text{NHCONH}-$	$-\text{CH}_2\text{CH}_2-$	$-\text{OCH}_2\text{CH}_2-$	R ₃ CH
10		$\text{H}_3\text{C}-\text{NHCSNH}-$	$-\text{CH}_2\text{CH}_2-$	$-\text{OCH}_2\text{CH}_2-$	R ₃ CH
11	TACN ^a	$-\text{CH}_2\text{NHCSNH}-$	$-\text{CH}_2\text{CH}_2-$	$-\text{OCH}_2\text{CH}_2-$	R ₃ CH
12	TACN ^a	$-\text{CH}_2\text{NHCONH}-$	$-\text{CH}_2\text{CH}_2-$	$-\text{OCH}_2\text{CH}_2-$	R ₃ CH
13	BzR ₃	$-\text{CH}_2\text{NHCSNH}-$	$-\text{CH}_2\text{CH}_2-$	$-\text{OCH}_2\text{CH}_2-$	R ₃ N
14	BzR ₃	$-\text{CH}_2\text{NHCONH}-$	$-\text{CH}_2\text{CH}_2-$	$-\text{OCH}_2\text{CH}_2-$	R ₃ N

^a 1,4,9-Triazacyclononane.

Ditopic Salt Binders L and Their Complexes L:NaCl.

A number of plausible ligands L (32 of them) were constructed, and their complexes L:NaCl were initially optimized at the HF/3-21G level. In general, two versions of each ligand have been considered, differing only by the substitution of sulfur for oxygen in the carbonyl of the amide groups of the anion-binding moiety. All of the ligands reported here contain alkyl group spacers; some of the early ligands employed benzyl spacers to make the cavity more rigid, but this tended to reduce the binding and/or distort the complex from C_3 symmetry. The structures of the ligands are summarized in Table 5; key geometrical details and binding energies are summarized in Tables 6 and 7, respectively. In the following discussion, we will focus on the DFT (BHandH) results (we note that the HF/6-31+G* equivalent to Table 6 is supplied as Supporting Information, Table 6S). The “raw” electronic and thermal energy data on which the quantities in Tables 1–7 are based are also provided as Supporting Information (Tables 1S–5S). The BhandH/6-31+G* geometry-optimized coordinates of all species are also provided in the Supporting Information (Tables 7S–62S).

The first pair of complexes to be stable and show the desired properties were 1:NaCl and 2:NaCl (Figure 2a,b), which employ a single $-\text{CONH}-$ or $-\text{CSNH}-$ amide/thioamide anion binding group and $-\text{CH}_2-\text{CH}_2-\text{CH}_2-$ spacer in each arm of the ligand. NaCl is clearly bound as a contact ion pair with a bond length $r(\text{Na}-\text{Cl}) \approx 2.37$ Å, almost identical to the gas-phase NaCl molecule at the same level of theory (Table 1). The NaCl binding energy of this ligand is 80 kJ/mol for the triamide **1** and 116 kJ/mol for the trithioamide **2**. Both HF and DFT levels of theory predict stronger binding for the thioamide ligand, and this turns out to be a consistent feature for all the successful pairs of amide/thioamide ligands. The H-bonding geometry of this ligand seems to be particularly favorable, with slightly shorter and more linear $\text{N}-\text{H}\cdots\text{Cl}$ contacts in 2:NaCl, consistent with its higher binding energy. However, the acute $\text{C}-\text{O}-\text{Na}^+$ angles (83° – 84°) at the cation-binding pocket of both ligands suggest a strained geometry this part of the ligand (this is 30° lower than the equivalent angles in the podand complex,

Table 6. BHandH/6-31+G* Geometry-Optimized Data for the Complexes L:NaCl

	$r(\text{H}\cdots\text{Cl}^-)$ (Å)	$\text{N}-\text{H}\cdots\text{Cl}^-$ (deg)	$r(\text{O}\cdots\text{Na}^+)$ (Å)	$r(\text{Na}\cdots\text{Cl})$ (Å)	$\text{C}-\text{O}\cdots\text{Na}^+$ (deg)	$q(\text{Na}^+)$ (au) ^a	$q(\text{Cl}^-)$ (au) ^a
1	2.177	143.1	2.255	2.368	82.8	+0.315	-0.959
2	2.124	146.2	2.239	2.374	83.8	+0.399	-1.007
3	3.228, 3.363	83.3, 73.1	2.211	2.383	91.2	+0.473	-0.686
4	2.591, 3.018	97.8, 88.1	2.275	2.325	82.4	+0.310	-1.076
5	2.465, 2.429	141.2, 136.0	2.155	2.393	107.6	+0.299	-0.605
6	2.461, 2.242	144.1, 151.2	2.152	2.401	104.6	+0.392	-0.616
7	2.445, 2.285	150.3, 159.0	2.166	2.453	112.8	+0.569	-0.643
8	2.401, 2.364	152.2, 157.3	2.179	2.476	112.8	+0.333	-0.588
9	2.367, 2.376	146.7, 147.8	2.226	3.448	124.2	+1.588	-0.681
10	2.314, 2.353	148.6, 150.6	2.237	3.134	121.7	+0.214	-0.642
11	2.533, 2.194	129.0, 142.0	2.156	2.391	107.6	+0.451	-0.697
12	2.525, 2.202	132.1, 145.7	2.147	2.384	107.8	+0.400	-0.671
13	2.235, 2.319	162.1, 157.5	2.279	2.527	106.4	+0.462	-0.787
14	2.253, 2.403	152.6, 161.8	2.276	2.523	107.5	+0.332	-0.726

^a Mulliken charges.**Table 7.** Binding Energies of Various Complexes at Different Levels of Theory (kJ/mol)

	HF/3-21G ^a			HF/6-31+G* ^a			BHandH/6-31+G* ^a		
	L:NaCl	L:Na ⁺	L:Cl ⁻	L:NaCl	L:Na ⁺	L:Cl ⁻	L:NaCl	L:Na ⁺	L:Cl ⁻
1	121.9	370.7	118.5	-18.8	171.9	91.0	77.8	228.9	180.8
2	185.1	326.7	211.5	13.6	135.2	147.2	116.0	195.4	236.7
3	135.8	414.9	45.3	-31.9	205.1	6.6	66.1	253.5	92.3
4	53.3	480.6	13.1	-83.9	308.0	30.8	26.8	375.9	116.4
5	256.1	565.2	204.0	98.4	362.2	171.3	199.8	418.5	264.4
6	281.9	444.9	274.8	114.2	308.6	207.9	214.7	364.9	294.8
7	330.0	463.9	260.0	172.0	309.0	191.1	271.1	390.3	293.5
8	314.0	397.0	212.2	165.0	255.8	171.0	269.9	311.2	272.6
9	387.6	435.2	199.3	208.5	294.6	187.5	285.5	328.3	218.0
10	404.3	466.0	291.6	214.2	297.0	229.2	338.4	407.2	296.9
11	257.8	433.6	216.6	83.2	238.9	154.8	185.6	361.9	247.5
12	189.4	420.0	115.7	70.5	259.2	125.7	126.1	309.8	176.1
13	365.9	494.2	232.5	206.0	326.5	165.0	320.6	456.5	277.5
14	368.9	503.4	207.1	215.7	311.9	172.0	327.4	416.4	268.2

^a Gas-phase binding energy including HF/3-21G thermal energies with the vibrational component scaled by 0.89.²¹

see Table 3). This suggests that the ligand cavity is too small; higher NaCl binding energies could be achieved if the sodium ion can relax further toward the center of the cavity.

It was reasoned that switching the anion-binding moiety to a urea/thiourea fragment ought to increase binding at the anion-binding end of L. A simultaneous reduction of the length of the spacer $-\text{CH}_2-\text{CH}_2-\text{CH}_2-$ should also have the effect of “pulling” the sodium ion toward the cavity center. These ideas were first tested in complexes **3**:NaCl and **4**:NaCl (Figure 2c,d). In **3**:NaCl which retains the longer (propyl) spacer, the urea groups are evidently too distant from the chloride anion to bind. Instead the Cl^- ion remains in close contact with Na^+ , $r(\text{Na}-\text{Cl}) \approx 2.38$ Å. However the strain at the cation binding pocket is partly removed, as the $\text{C}-\text{O}-\text{Na}^+$ angles increases to 92° . In **4**:NaCl, removing one methylene group from each spacer and reinserting it between the urea groups and the R_3CH cap does facilitate $\text{N}-\text{H}\cdots\text{Cl}^-$ hydrogen bond formation for the half of the urea fragments; but the other remaining urea $\text{N}-\text{H}$ bonds are still too far from Cl^- to engage in hydrogen bonding, and the $\text{C}-\text{O}-\text{Na}^+$ angles are once again acute at $\approx 83^\circ$. The NaCl binding energies of 66 and 27 kJ/mol for **3**:NaCl and **4**:NaCl, respectively, are very low, and the fact that **3** binds more strongly than **4** despite the presence of weak $\text{N}-\text{H}\cdots\text{Cl}^-$ hydrogen bonds in the latter suggests that the partial removal

of strain in the cation pocket of **3**:NaCl was energetically a more important consideration.

One of the striking features of complexes **3**:NaCl and **4**:NaCl is that the $\text{N}-\text{H}$ bonds of the urea moieties point away from the center of the cavity. This led us to conclude that the $\text{HC}(\text{CH}_2)_3$ anion binder cap is too small to permit effective urea... Cl^- binding. Several possible alternative cap functional groups with potential C_3 symmetry were explored at this point, including cyclohexyl and triazacyclohexyl groups, but the HF/3-21G optimized structures were strongly distorted from C_3 and furthermore did not improve the anion binding. The benzyl and triazacyclononyl groups were much more successful, and these are discussed below.

In complexes **5**:NaCl and **6**:NaCl (Figure 2e,f) the urea/thiourea anion-binding moieties are bonded to a 1,3,5-trisubstituted benzyl spacer, $\text{C}_6\text{H}_3(\text{CH}_2)_3$. It is immediately apparent that this has the effect of opening up the anion binding end of the cavity to the extent that six $\text{N}-\text{H}\cdots\text{Cl}^-$ hydrogen bonds are formed in both amide and thioamide versions of the ligand. The geometry at the Na^+ cation has also become much more favorable for optimal binding, with $\text{C}-\text{O}-\text{Na}^+$ angles of 108° (105° in the trithiourea ligand). Despite the presumably much stronger binding of Cl^- , the NaCl moiety remains as an ion contact pair with bond length $r(\text{Na}-\text{Cl}) \approx 2.4$ Å. The overall NaCl binding energies of

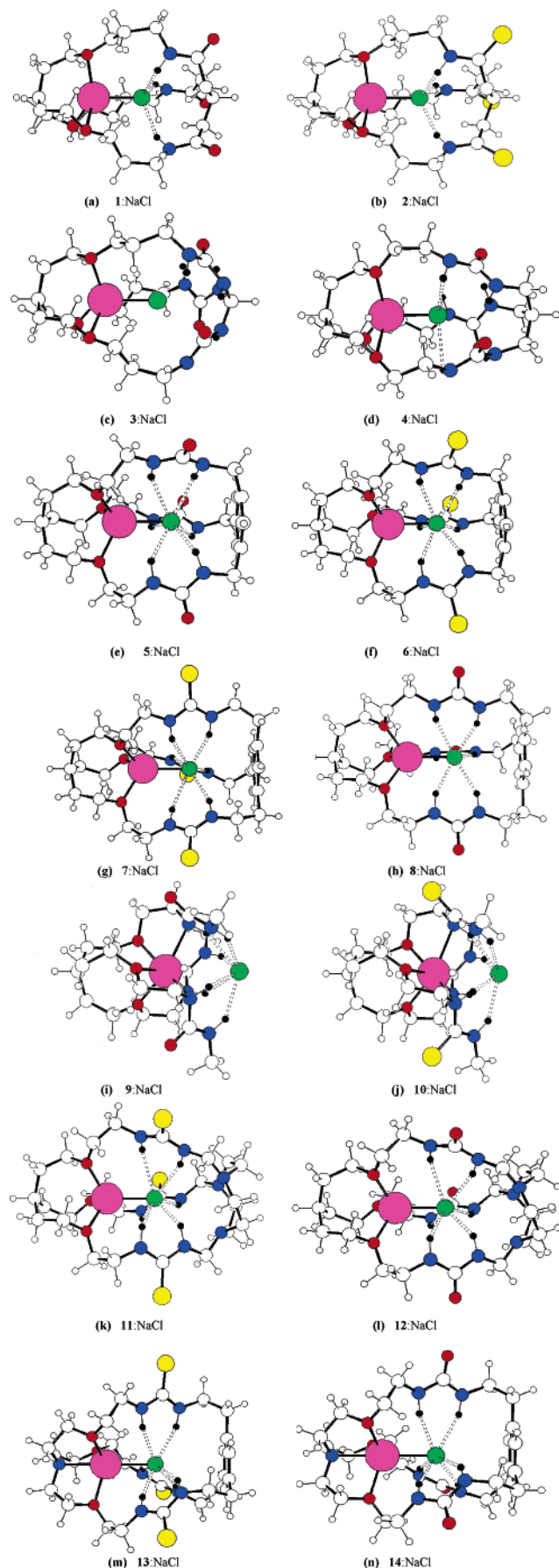


Figure 2. BHandH/6-31+G* geometry-optimized structures of the $L:\text{NaCl}$ complexes (L = hosts 1–14 as described in the main text).

200 kJ/mol (215 kJ/mol for the trithiourea ligand) show a substantial improvement over the previous candidate ligands. Thus it appears that this is already an excellent candidate for a ditopic NaCl binding ligand. We note however that the hydrogen bonding geometry at Cl^- could still bear some optimization: the $\text{H}\cdots\text{Cl}^-$ distances in the triurea ligand are quite long at ≈ 2.45 Å (much more asymmetric in the trithiourea with 2.46 Å and 2.24 Å), and the $\text{N}-\text{H}\cdots\text{Cl}^-$ angles are still generally below 150° . Careful inspection of Figure 2e,f also shows that the benzyl caps appear to be in slightly strained (nonplanar) geometries which probably decrease the effective NaCl binding energies of the complexes.

In 7:NaCl and 8:NaCl the effect of further expanding the cavity at the anion-binding pocket has been explored by including an extra methylene spacer in the anion binding cap, which is now $\text{C}_6\text{H}_3(\text{CH}_2\text{CH}_2)_3$. The details of the hydrogen bonding geometries in Table 6 for both the urea and thiourea complexes show that this has been effective: the H-bonds are shorter in the trisurea case (although not much different to 6:NaCl for the trithiourea complex 7:NaCl); but all $\text{N}-\text{H}\cdots\text{Cl}^-$ angles are now above 150° (i.e. more linear) in both complexes. The benzyl fragments are now quite planar. The $\text{C}-\text{O}-\text{Na}^+$ angles of $\approx 113^\circ$ are very close to the value of $\approx 116^\circ$ found for the podand complex $\text{H}(\text{CH}_2\text{CH}_2\text{OMe})_3:\text{Na}^+$, which suggests that ligands 7 and 8 have a close-to-ideal geometry for the Na^+ binding pocket. A substantial increase in overall NaCl binding energy is again seen, and this time the urea and thiourea complexes give almost identical binding (≈ 270 kJ/mol).

The complexes 9:NaCl and 10:NaCl represent our only departures from a closed bicyclic cage design—here we have explored the effect of an open-ended anion-binding moiety, i.e., a podand instead of a cryptand. Examining the geometry-optimized structures (Figure 2i,j) it is immediately evident that these complexes are qualitatively different to all the others: the $r(\text{Na}-\text{Cl})$ separation has stretched well beyond the gas-phase value of Å, reaching 3.45 Å in the carbonyl complex. Another feature unique to this pair of complexes is that the sodium cation is η^6 -coordinated, with the nitrogens of adjacent urea/thiourea groups acting as electron donors. This fundamental change in cation coordination results in Mulliken charges which are quite out of line with the 0.3–0.6 range seen in all other complexes: an extremely high $q(\text{Na}^+) = +1.59$ for 9:NaCl and paradoxically the lowest value seen, $q(\text{Na}^+) = +0.24$ for 10:NaCl. In short, the effect of opening the cavity at the anion-binding end has produced a ditopic binder in which the Na^+ and Cl^- ions are no longer a contact pair, due to the moreover, this effect is accompanied by a substantial increases in overall binding energy (288 and 338 kJ/mol). We note however that the anion in these open-ended complexes would not be effectively shielded from solvent molecules, so it is questionable whether this exceptionally high binding energy would actually be achieved in the aqueous phase.

In 11:NaCl and 12:NaCl the effect of replacing the trisubstituted benzyl spacer with a $\text{N},\text{N}',\text{N}''$ -functionalized triazacyclononane is explored. This is a common ligand in coordination chemistry.²⁶ We consider it here on the basis of its potential C_3 symmetry as a design element in these

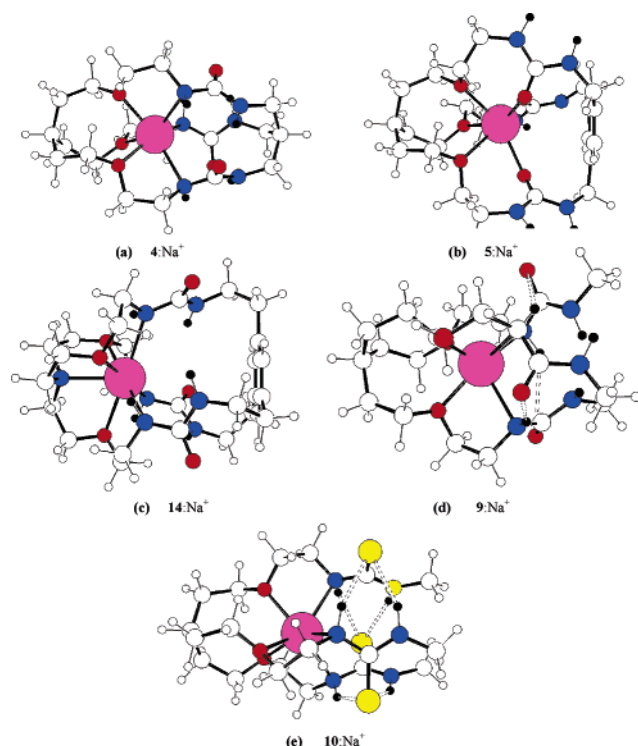


Figure 3. BHandH/6-31+G* geometry-optimized structures of selected complexes $L:Na^+$, illustrating the different modes of coordination obtained.

ligands, and because of its well-known utility in supramolecular design. It was found that, although the complexes $11:NaCl$ and $12:NaCl$ were stable in C_3 , the free ligands distorted considerably to C_1 . (For the 14 ligands reported in this paper, **11** and **12** are the only cases where the *free* ligands are not C_3 -symmetric.) In the complexes with $NaCl$, the introduction of the TACN functionality has an adverse effect on the hydrogen bonding geometry, with less linear and generally longer hydrogen bonds than those of the previously discussed complexes. The much lower binding energies of 186 kJ/mol (trithioamide) and 126 kJ/mol (triamide) presumably reflect this poorer H-bonding geometry.

In $13:NaCl$ and $14:NaCl$ the effect of adding an additional coordination site for the sodium cation is explored, by simply replacing the axial CH of the cation binding caps of **7** and **8** with a nitrogen heteroatom. It might also be argued that such ligands are easier to synthesize than some of the preceding ones, using e.g. triethanolamine as a starting material. The optimized structures (Figure 2m,n) demonstrate that the sodium ion is indeed η^4 -coordinated, and the complexes retain C_3 symmetry. Although the $Na\cdots Cl$ contact distances are slightly longer in these complexes, $r(Na-Cl) \approx 2.53$ Å, the anion binding is not at all adversely affected; in fact the $N-H\cdots Cl$ H-bonds are some of the shortest and are closer to being linear than any of the other the complexes reported here. The $NaCl$ binding energies for this pair of ligands are very similar and are the largest obtained for any of the ligands *except* for the podand complex $10:NaCl$.

The Complexes $L:Na^+$. The η^6 -coordination Na^+ mode which was found only in the two podand ditopic complexes $9:NaCl$ and $10:NaCl$ is in fact seen in a number of the complexes of these ligands with just a sodium cation (**4**:

Na^+ , **5**: Na^+ , **7**: Na^+ , **9**: Na^+ , **10**: Na^+ , **11**: Na^+ , and **12**: Na^+). Two representative examples **4**: Na^+ and **5**: Na^+ are shown in Figure 3a,b. Figure 3a depicts the first type of coordination, involving the three ether oxygens and three nitrogen atoms of the urea groups; this occurs in **4**: Na^+ , **9**: Na^+ , **10**: Na^+ , **11**: Na^+ , and **12**: Na^+ . Figure 3b depicts a second type of coordination seen in two cases (**5**: Na^+ and **7**: Na^+) where carbonyl(thiocarbonyl) oxygens(sulfurs) are acting as additional donors. Where it occurs, the switch from η^3 - to η^6 -coordination is unsurprisingly accompanied by an increase in $L:Na^+$ binding energy (for example, the 376 kJ/mol binding energy of **4**: Na^+ is much higher than the 254 kJ/mol value for η^3 -coordinated **3**: Na^+), and this explains most trends seen in Table 5. Complexes **13**: Na^+ and **14**: Na^+ actually have η^7 -coordination at Na^+ due to the extra capping nitrogen heteroatom (see the example in Figure 3c). Another feature which also enhances the stability of several complexes (**4**: Na^+ , **9**: Na^+ , **10**: Na^+ , **12**: Na^+ , and **13**: Na^+) is the formation of intramolecular $N-H\cdots O$ or $N-H\cdots S$ hydrogen bonds: the example (two examples are shown in Figure 3d,e). We note that, in general, the best ditopic $NaCl$ binders also happen to be the best binders for Na^+ alone, based on these gas-phase binding energy considerations.

The Complexes $L:Cl^-$. The full H-bonding geometrical data for these complexes are reported in Table 7S. Although **1**: Cl^- and **2**: Cl^- only form three $N-H\cdots Cl$ H-bonds, these bonds are quite linear and short (see Figure 3a), hence the chloride binding energies of 181 and 236 kJ/mol (the latter for the thiourea species) are fairly high. The complex **3**: Cl^- is the ‘odd one out’ because $N-H\cdots Cl$ hydrogen bonds do not form at all due to competing $N-H\cdots O$ (carbonyl) hydrogen bonding interactions (see Figure 3b), so unsurprisingly its chloride binding energy is the lowest. Of the remaining complexes, **5**: Cl^- , **6**: Cl^- , **7**: Cl^- , **8**: Cl^- , **11**: Cl^- , **12**: Cl^- , **13**: Cl^- , and **14**: Cl^- are all fairly similar in that they contain three pairs of $N-H\cdots Cl$ H-bonds with geometries ranging from $N-H\cdots Cl = 124^\circ - 165^\circ$ and $r(H\cdots Cl)$ ranging from 2.21 Å to 2.51 Å. So although the “ideal” H-bonding distance of 2.17 Å (from the *N,N*-dimethylthiourea: Cl^- complex) is never quite attained for these various bicyclic ligands, several have $N-H\cdots Cl^-$ angles higher than the 158° obtained for *N,N*-dimethylthiourea: Cl^- . The thiourea versions of these ligands have consistently higher chloride binding energies than their urea-based equivalents, the strongest complex being found for **6**: Cl^- (shown in Figure 3c). The two remaining (podand) complexes **9**: Cl^- and **10**: Cl^- also bind chloride strongly (in fact **10**: Cl^- has an almost identical binding energy to **6**: Cl^- , see Figure 4), but both have strongly distorted to C_1 symmetry (see Figure 3d).

Discussion – Quantitative Structure–Property Relationships

The parameters listed in Table 6 have been used to construct various quantitative structure–property relationships using least-squares models of the BHandH/6-31+G* binding energies for the complexes $L:NaCl$. After some experimentation we found that the most efficient linear model of the binding energy is a three-parameter model involving one distance $r(O\cdots Na^+)$, which we will denote as d , and two

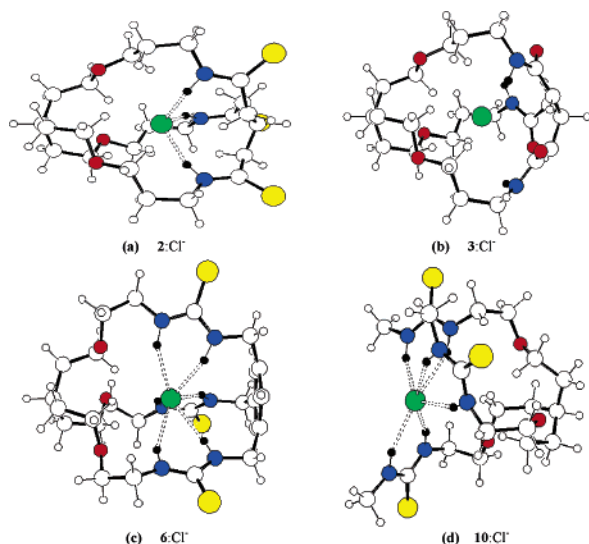


Figure 4. BHandH/6-31+G* geometry-optimized structures of selected complexes $L:Cl^-$, illustrating the different modes of coordination obtained.

angles: $N-H\cdots Cl^-$ and $C-O\cdots Na^+$, which will be denoted as θ and ω , respectively

$$BE(\theta, d, \omega) \approx -2015.1 + 1.636 \theta + 632.41 d + 5.699 \omega \text{ kJ/mol} \quad (5)$$

where the distance d is in Å and the angles are in degrees. This model delivers an R^2 value of 0.91 and an rms error on the predicted binding energy of 36.2 kJ/mol for all 14 data. The remaining parameters, including the $r(Na\cdots Cl)$ separation and the partial (Mulliken) charges $\{q(Na^+), q(Cl^-)\}$ do not appear to play an important role in determining the binding energy and are also strongly linearly correlated with the three parameters in (5).

Although eq 5 provides a rough estimate of the ion pair binding energy for a given structure, the coefficients in this linear model have no physical significance. We hypothesize that there is some *optimal* cavity size and shape which will lead to the highest possible ion pair binding energy. This must be strictly true if **1–14** all contained an identical arrangement of binding heteroatoms but differed only in the size and shape of the binding pocket. This is not strictly the case for our molecules, for several reasons: (i) some molecules contain ureas while others contain thioureas; (ii) **1** and **2** have amide/thioamide groups instead of ureas or thioureas; and (iii) **11** and **12** have an additional capping nitrogen atom which also plays a role in cation binding. We can nevertheless explore this hypothesis by attempting to fit the simplest nonlinear model to the ion pair binding energies which is consistent with the notion of an optimal cavity size/shape. So we choose the same three structural parameters which were indicated to be most important from the linear model and rewrite the binding energy in quadratic form

$$BE(\theta, d, \omega) \approx BE_{\max} - k_1(\theta - \theta_0)^2 - k_2(d - d_0)^2 - k_3(\omega - \omega_0)^2 \quad (6)$$

where BE_{\max} represents the maximum achievable binding energy; $\{k_1, k_2, k_3\}$ are pseudoforce constants; and $\{\theta_0, d_0,$

$\omega_0\}$ represent “optimal” values of these three structural parameters. Although there are seven parameters in this model, using Mathematica⁵²⁸ we find that it is possible to obtain a stable fit of eq 6 to our 14 ion pair binding energies:

$$BE \approx 353.24 - 0.011 (\theta - 179.6)^2 - 9553.5 (d - 2.268)^2 - 0.219 (\omega - 116.1)^2 \text{ kJ/mol} \quad (7)$$

Equation 7 approximates the exact BhandH/6-31+G* ion pair binding energies with an rms error of 21 kJ/mol; moreover, the fitted parameters have a direct physical interpretation. The suggested optimal values are revealing. The $r(O\cdots Na^+)$ distance of ≈ 2.27 Å is attained in two of our complexes (**13:NaCl** and **14:NaCl**), but in most of them it is significantly shorter. The optimal $C-O\cdots Na^+$ angle is almost identical to the value obtained for $HC(CH_2CH_2OMe)_3:Na^+$ at the same level of theory; this angle is several degrees lower in all but two of our complexes (**9:NaCl** and **10:NaCl**). Finally, the optimal $N-H\cdots Cl^-$ angle is suggested to be as close to 180° as possible. These observations taken together suggest that it would be beneficial to further increase the size of the NaCl binding pocket. However, because the fitted value of BE_{\max} is only 15 kJ/mol higher than our best value (for **10:NaCl**), the increase in binding energy following this modification would probably be limited.

We also considered linear models of the $L:Cl^-$ binding energy. (We did not attempt to model the $L:Na^+$ binding energy because of the considerable variation in binding modes seen across the 14 compounds). For the $L:Cl^-$ complexes, linear models do not appear to be very useful, the best (two-parameter) model involving $r(H\cdots Cl)$ and $N-H\cdots Cl$ delivers only $R^2 = 0.797$ and an rms error of 32.4 kJ/mol for all 14 data.

Conclusions

The preliminary studies of model anion and cation binding systems showed that ditopic binders are challenging systems for quantum chemical calculations. Density functional methods are currently the only way forward for systems of this size, if electron correlation effects are to be taken into account, but choosing a density functional which accounts for both anion-binding and cation-binding interactions with similar accuracy is problematic. Nevertheless, we believe that this study has led to a number of important conclusions regarding the design of potential ditopic salt binding ligands.

(i) It certainly is possible to design cryptand-like, C_3 -symmetric cages with adjacent anion and cation binding sites leading to very strong ion pair binding (binding energies in excess of 300 kJ/mol relative to free NaCl). A systematic design process using quantum chemical methods has provided several excellent candidate host molecules. An ethyl spacer between anion- and cation-binding pockets was found to be optimal for maximizing the anion–cation interaction. The introduction of a *rigid* anion binder cap in the form of a 1,3,5-trisubstituted benzene proved to be essential in providing the correct spacing for the ureas/thioureas to bind effectively to the chloride.

(ii) Thioamides and thiourea are generally better ligands for Cl^- binding than the equivalent amide and urea ligands, which up to this point have been preferred synthetically. This is probably linked to our observation that Cl^- :dimethylthiourea complexes seem to prefer a more coplanar geometry than the analogous Cl^- :dimethylurea complexes (i.e. this facilitates stronger H-bonds).

(iii) A nitrogen heteroatom for the cation-binding pocket also plays a role in cation binding. An equivalent neutral, C_3 -symmetric capping moiety for the anion-binding end of the host molecule might be *s*-triazine, which according to Frontera et al. has significant $\text{Cl}^- \cdots \pi$ interactions.^{13,21} We have not attempted any calculations using this fragment as an anion-binding cap because of the uncertainty associated with how well dft methods can model the relatively exotic halide anion $\cdots \pi$ interactions.

(iv) The size and shape of the cavity in which the anion and cation sit is also crucial for optimizing the NaCl binding energy. Although selectivity for NaCl over other ion pairs has not been explicitly considered here, it seems likely that our best bicyclic host **14** would be selective for NaCl because of the considerable time spent tuning the cavity size for this particular pair of ions during the design process.

(v) Trends in binding energies of the associated $\text{L}:\text{Na}^+$ and $\text{L}:\text{Cl}^-$ complexes are complex because coordination modes of the ions are not consistent across the series of compounds. It was originally anticipated that the difference between $\text{BE}(\text{L}:\text{NaCl})$ and the sum of $\text{BE}(\text{L}:\text{Na}^+)$ and $\text{BE}(\text{L}:\text{Cl}^-)$ could be used to measure of ‘cooperativity effects’ for the binding of the ion-pair: but this is not effective because of these complicated trends in the series $\text{BE}(\text{L}:\text{Na}^+)$ and $\text{BE}(\text{L}:\text{Cl}^-)$, due to varying coordination modes.

We should finally add a word on the synthetic feasibility of the ditopic hosts we have designed. The nitrogen-capped polyether podand form of our optimal system is already familiar from the very well-developed field of cryptand chemistry²⁷ (and we note that suitable starting products such as triethanolamine are off-the-shelf chemicals). At the anion-binding end of the system, the podand based on a 1,3,5-trithiourea substituted benzene is not (to our knowledge) a known ligand, but functionalizing benzyl groups with ureas is fairly straightforward and has been utilized in known ditopic binders such as the one mentioned earlier by Reinhoudt and co-workers.⁵ The “strapping” of these two elements to make the bicyclic system may not be at all trivial but could again draw on the very extensive knowledge base on this topic that has already been accumulated by researchers in the cryptand field.

Acknowledgment. S.T.H. and D.E.H. thank the Australian Research Council for funding (Grant DP0556144).

Supporting Information Available: HF/6-31+G* equivalent to Table 6 (Table 6S), the “raw” electronic and thermal energy data on which the quantities in Tables 1–7 are based (Tables 1S–5S), and BhandH/6-31+G* geometry-optimized coordinates of all species (Tables 7S–62S). This material is available free of charge via the Internet at <http://pubs.acs.org>.

References

- (1) Kirkovits, G. J.; Shriver, J. A.; Gale, P. A.; Sessler, J. L. *J. Incl. Phenom. Mac. Chem.* **2001**, *41*, 69–75.
- (2) Gale, P. A. *Coord. Chem. Rev.* **2003**, *240*, 191–221.
- (3) Bretag, A. *Life Sci.* **1969**, *8*, 319–329.
- (4) Rosenstein, B. J.; Zeitlin, P. L. *Lancet* **1998**, *351*, 277–282.
- (5) (a) Gao, L.; Broughman, J. R.; Iwamoto, T.; Tomich, J. M.; Venglarik, C. J.; Forman, H. J. *Am. J. Physiol. Lung Cell Mol. Physiol.* **2001**, *281*, L24–L30. (b) Jiang, C.; Lee, E. R.; Lane, M. B.; Xiao, X.-F.; Harris, D. J.; Cheng, S. H. *Am. J. Physiol. Lung Cell Mol. Physiol.* **2001**, *281*, L1164–L1172. (c) Rodgers H. C.; Knox, A. J. *Eur. Respir. J.* **2001**, *17*, 1314–1321.
- (6) Scheerder, J.; van Duynhoven, J. P. M.; Engbersen, J. F. J.; Reinhoudt, D. N. *Angew. Chem., Int. Ed. Engl.* **1996**, *35*, 1090–1093.
- (7) Koulov, A. V.; Mahoney, J. M.; Smith, B. D. *Org. Biomol. Chem.* **2003**, *1*, 27–29.
- (8) Mahoney, J. M.; Stucker, K. A.; Jiang, H.; Carmichael, I.; Brinkmann, N. R.; Beatty, A. M.; Noll, B. C.; Smith, B. D. *J. Am. Chem. Soc.* **2005**, *127*, 2922–2928.
- (9) Aldridge, S.; Fallis, I. A.; Howard, S. T. *Chem. Comm.* **2001**, 231–232.
- (10) Andreadakis, G. E.; Moschoul, E. A.; Matthaiou, K.; Froudakis, G. E.; Chaniotakis, N. A. *Anal. Chim. Acta* **2001**, *439*, 273–280.
- (11) Pichierri, F. *J. Mol. Struct. (THEOCHEM)* **2002**, *581*, 117–127.
- (12) Kim, S. K.; Singh, N. J.; Kim, S. J.; Kim, H. G.; Kim, J. K.; Lee, J. W.; Kim, K. S.; Yoon, J. *Org. Lett.* **2003**, *5*, 2083–2086.
- (13) Yoon, J.; Kim, S. K.; Singh, N. J.; Lee, J. W.; Yang, Y. J.; Chellappan, K.; Kim, K. S. *J. Org. Chem.* **2004**, *69*, 581–583.
- (14) Garau, C.; Quinonero, D.; Frontera, A.; Costa, A.; Ballester, P.; Deya, P. M. *Chem. Phys. Lett.* **2003**, *370*, 7–13.
- (15) Ruangpornvisuti, V. *J. Mol. Struct. (THEOCHEM)* **2004**, *686*, 47–55.
- (16) Brynda, M.; Tomasz A. Wesolowski, T. A.; Wojciechowski, K. *J. Phys. Chem. A* **2004**, *108*, 5091–5099.
- (17) Vivas-Reyes, R.; De Proft, F.; Biesemans, M.; Willem, R.; Geerlings, P. *Eur. J. Inorg. Chem.* **2003**, 1315–1324.
- (18) Mohamadi, F.; Richards, N. G. J.; Guida, W. C.; Liscamp, R.; Lipton, M.; Caufield, C.; Chang, J. C.; Hendrickson, T.; Still, W. C. *J. Comput. Chem.* **1990**, *11*, 440–449.
- (19) Hout, R. F.; Levi, B. A.; Hehre, W. J. *J. Comput. Chem.* **1982**, *3*, 234–241.
- (20) Frisch, M. J.; Trucks, G. W.; Schlegel, H. B.; Scuseria, G. E.; Robb, M. A.; Cheeseman, J. R.; Montgomery, J. A., Jr.; Vreven, T.; Kudin, K. N.; Burant, J. C.; Millam, J. M.; Iyengar, S. S.; Tomasi, J.; Barone, V.; Mennucci, B.; Cossi, M.; Scalmani, G.; Rega, N.; Petersson, G. A.; Nakatsuji, H.; Hada, M.; Ehara, M.; Toyota, K.; Fukuda, R.; Hasegawa, J.; Ishida, M.; Nakajima, T.; Honda, Y.; Kitao, O.; Nakai, H.; Klene, M.; Li, X.; Knox, J. E.; Hratchian, H. P.; Cross, J. B.; Adamo, C.; Jaramillo, J.; Gomperts, R.; Stratmann, R. E.; Yazyev, O.; Austin, A. J.; Cammi, R.; Pomelli, C.; Ochterski, J. W.; Ayala, P. Y.; Morokuma, K.; Voth, G. A.; Salvador, P.; Dannenberg, J. J.; Zakrzewski, V. G.; Dapprich,

- S.; Daniels, A. D.; Strain, M. C.; Farkas, O.; Malick, D. K.; Rabuck, A. D.; Raghavachari, K.; Foresman, J. B.; Ortiz, J. V.; Cui, Q.; Baboul, A. G.; Clifford, S.; Cioslowski, J.; Stefanov, B. B.; Liu, G.; Liashenko, A.; Piskorz, P.; Komaromi, I.; Martin, R. L.; Fox, D. J.; Keith, T.; Al-Laham, M. A.; Peng, C. Y.; Nanayakkara, A.; Challacombe, M.; Gill, P. M. W.; Johnson, B.; Chen, W.; Wong, M. W.; Gonzalez, C.; Pople, J. A. Gaussian, Inc.: Pittsburgh, PA, 2003.
- (21) Huber, K. P.; Herzberg, G. Molecular Spectra and Molecular Structure. In *Constants of Diatomic Molecules*; Van Nostrand: New York, 1979; Vol. IV.
- (22) Garau, C.; Frontera, A.; Ballester, P.; Quinonero, D.; Costa, A.; Deya, P. M. *Eur. J. Org. Chem.* **2004**, 1, 179–183.
- (23) Sun, H.; Kung, P. W. C. *J. Comput. Chem.* **2005**, 26, 169–174.
- (24) Bencivenni, L.; Cesaro, S. N.; Pieretti, A. *Vib. Spectrosc.* **1998**, 18, 91–102.
- (25) (a) Buhl, M.; Ludwig, R.; Schurhammer, R.; Wipff, G. *J. Phys. Chem. A* **2004**, 108, 11463–11468. (b) Anderson, J. D.; Paulsen, E. S.; Dearden, D. V. *Int. J. Mass Spectr.* **2003**, 227, 63–76. (c) Glendening, E. D.; Feller, D. *J. Am. Chem. Soc.* **1996**, 118, 6052–6059.
- (26) Wainwright, K. P. *Coord. Chem. Rev.* **1997**, 166, 335–90.
- (27) Menon, S. K.; Hirpara, S. V.; Harikrishnan, U. *Rev. Anal. Chem.* **2004**, 23, 233–267.
- (28) Wolfram Research, Inc. *Mathematica Version 5.2*; Wolfram Research, Inc.: Champaign, IL, 2005.

CT050270D